Production and Characterization of Nanoencapsulated Phase Change Materials (PCMs) and Bicomponent PCM Nanofibers

Simge ÖZKAYALAR, 0000-0002-5390-8317
Sennur ALAY AKSOY* 0000-0002-5878-6726

Süleyman Demirel University, Engineering Faculty, Textile Engineering Department, Isparta, Turkey

Corresponding Author: Sennur Alay Aksoy, sennuralay@sdu.edu.tr

ABSTRACT

The aim of this study was to fabricate the nanocapsules and nanofibers with latent heat energy storage properties. Therefore, phase change materials based on fatty alcohols were used as latent heat energy storage materials. N-Dodecanol and 1-tetradecanol fatty alcohols were nanoencapsulated by poly(methyl methacrylate-co-methacrylic acid) (p(MM-co-MA)) wall using emulsion polymerization method. Prepared nanocapsules were incorporated in polyacrylonitrile nanofibers using the co-axial electrospinning method. In this study, a two-stage (TS) emulsion polymerization process was defined and compared to the known emulsion polymerization method defined as one-stage (OS). Nanocapsules were characterized by Fourier-transform infrared (FT-IR) spectroscopy, transmission electron microscopy (TEM), differential scanning calorimeter (DSC), and thermogravimetric analyzer (TGA). According to the results, typical core-shell structured, spherical-shaped, uniform nano-sized particles having high thermal stability and energy storage capacity were fabricated successfully. Enthalpy values of the nanocapsules prepared by the TS process were higher and reached up to 171 J/g. It was concluded that the thermal degradation stability of the nanocapsules could be improved using the TS emulsion polymerization method. Moreover, the nanocapsules were incorporated in polyacrylonitrile nanofibers using the co-axial electrospinning method, and composite nanofibers having 19 J/g energy storage capacities were produced. Although the surfaces of the prepared core-sheath structured nanofibers were rough and coarse, their diameter distribution was unimodal.

1. INTRODUCTION

Phase change materials (PCMs) have attracted a great deal of attention because of their capability of storing and releasing large amounts of latent heat during their phase change from one physical state to another. They have been used as an energy storage material in many fields such as solar energy storage, energy-efficient buildings, thermoregulation clothing, and industrial textiles due to their high energy storage capacity. A large number of organic and inorganic solid-liquid PCMs are available. Organic-based PCMs such as paraffin waxes or n-alkanes, polyethylene glycol, fatty acids generally have been preferred as thermal energy storage materials in many end-use fields [1]. Their phase change temperatures and energy storage capacities have taken into account in this selection. One type of organic-based PCMs is fatty alcohols such as n-dodecanol and 1-tetradecanol. In recent years, the use of fatty alcohols as thermal energy storage material has been attracted great deal of interest because of their low cost than paraffin waxes and having high heat density and a wide range of melting temperatures. However, fatty alcohols have some disadvantages such as leakage, subcooling, low thermal conductivity, reactivity toward the outside environment, and flammability [2]. To overcome these disadvantages, encapsulation technology has been utilized. Encapsulation is to packet an oil drop or a solid particle as a

core material in a wall in order to develop micro or nano-sized capsules [3]. Encapsulated PCM is composed of a PCM as the core, and a polymer or an inorganic shell to maintain the spherical capsule shape and prevent leakage of PCM during its melting [4, 5]. The wall structure plays very important role in order to meet the requirements of the usage area of the encapsulated PCMs. According to the literature survey on usage of fatty alcohols as PCM, n-dodecanol have been encapsulated by various wall materials such as SiO_2 [2], melamine-formaldehyde resin [6-8], methanol–melamine-formaldehyde [9, 10], styrene-butyl acrylate copolymer [11], polymethyl methacrylate (PMMA) [12], acrylic-based copolymer prepared using acrylic monomers such as polyurethane acrylate and 1,4-butylene glycol diacrylate [13], graphene oxide-modified poly(melamine-formaldehyde) [14], poly(methyl methacrylate) copolymer with different type co-monomers such as acrylamide, butyl acrylate and acrylic acid [15], poly(allyl methacrylate) [16], melamine–urea-formaldehyde resins [17].

In the textile industry, phase change materials are used to improve thermal clothing comfort and produce smart thermo-regulating textiles. They have been incorporated into the fibers directly or encapsulated form, during the fiber spinning. Additionally, coating the fabrics with encapsulated PCM doped polymer has been realized. Recently, the electrospinning technique has been utilized to produce nano-sized form-stable phase change fibers containing PCMs in a supporting polymer matrix [18, 19]. Electrospinning technique has been used to fabricate the phase change-composite fibers with unique advantages such as ultrafine size, huge surface-to-volume ratio, excellent thermal performance, lightweight, and direct useage in various composites [18, 20, 21]. Electrospinning is a simple and versatile method that involves the usage of electrostatic force to draw a polymer solution into fibers whose diameters vary from a few nanometers to a submicron scale [18, 22, 23]. Phase change-composite nanofiber webs prepared by single and double nozzle (coaxial) electrospinning techniques can be applied in garments, electronic components, etc. in order to enhance the efficiency of thermal regulation [20]. Recently, the preparation of temperature-regulating composite nanofibers by coaxial electrospinning technique has attracted more and more attention. In coaxial electrospinning, concentrically aligned spinnerets have been used to fabricate core-sheath or hollow nanofibers [22, 24]. Coaxial electrospinning is a promising method to encapsulate PCM in the core of the fibers and to maintain it inside the polymer sheath layer of the fibers [25]. Coaxial electrospinning offers encapsulation of both hydrophilic and oleophilic PCMs in a variety of polymers and enhances the mechanical properties of the phase-change-composite nanofibers [21]. Oleophilic or hydrophilic solid-liquid PCMs such as long-chain hydrocarbons and polyethylene glycol have been encapsulated in core-sheath structured nanofibers by coaxial electrospinning method [21, 24-32].

The aim of this study is to produce the nanocapsules and nanofibers having latent heat storage and release properties with improved thermal properties. In literature, poly(methyl methacrylate) (PMMA) and its copolymers have been used in the encapsulation of the various solid-liquid PCMs such as n-alkanes and fatty acids [33-39]. In this study, n-dodecanol and 1-tetradecanol fatty alcohols were used as solid-liquid phase-change materials and nanoencapsulated in the wall of poly(methyl methacrylate-co-methacrylic acid) (p(MMA-co-MA)). A two-stage emulsion polymerization process was performed to investigate its performance in improving the thermal stability of the capsule shell structure. In the TS emulsion polymerization process, the methacrylic acid monomer was added to the emulsion medium during the second stage of the process. Thereby, firstly PMMA shell was synthesized to produce nanocapsules having a poly(methyl methacrylate) inner shell. In the second step of the process, MMA and MA monomers were copolymerized to produce a poly(methyl methacrylate-co-methacrylic amide) outer shell structure. Additionally, it was aimed to form the nanocapsule shell containing more numerous functional carboxylic acid groups by increasing the MA monomer in the outer surface of the nanocapsules. Thereby, the homogeneous distribution of the nanocapsules in the PEG solution, which was the core spinning solution of the bicomponent nanofibers, was aimed by increasing molecular interaction between the OH groups of PEG and carboxylic acid groups of the MA. In the study, synthesis of the single P(MMA-co-MA) shell was carried out using the conventional emulsion polymerization method which was defined as one-stage emulsion polymerization. Their properties were compared to the TS nanocapsules. The prepared TS nanocapsules were loaded in nanofibers as the core material via co-axial electrospinning technique and the placement of the nanocapsules in the fiber structure was investigated.

2. MATERIAL AND METHOD

2.1 Material

Methyl methacrylate (MMA, Merck) and methacrylic acid (MA, from Sigma Aldrich) were used as monomers to synthesize the shell of the nanocapsules. Ethylene glycol dimethacrylate (EGDM, from Merck Company) was used as a cross-linker. n-Dodecanol and (from Sigma Aldrich) 1-tetradecanol (from Merck) as PCMs, and Triton X-100 (from Sigma Aldrich) as an emulsifier were used. Ferrous sulfate heptahydrate and ammonium persulfate used as initiators were obtained from a Sigma Aldrich company. Sodium thiosulfate (from Merck) was used as a reactive material. Tert-butyl hydroperoxide (70 % in water) was obtained as an initiator from Acros Organics Company and used as received.

To produce nanofibers, polyacrylonitrile (PAN, Mw 150000 g/mole from Sigma Aldrich) and polyethylene glycol (PEG, Mw 1000 g/mol from Alfa Aesar) were used as polymers. N,N-Dimethylformamide (DMF, with a purity of > % 98.8 from Carlo Erba Reagent) was used as the solvent.

2.2 Method

2.2.1. Preparation of the nanocapsules

In this study, encapsulation of n-dodecanol and 1-tetradecanol was carried out by emulsion polymerization method. Different from the studies in literature, the emulsion polymerization process (two-stage) was carried out in two steps to manufacture nanocapsules having poly(methyl methacrylate) inner and poly(methyl methacrylate-co-methacrylic acid) outer walls.

In a two-stage (TS) polymerization procedure, a 12.5 g quantity of core material (n-dodecanol or 1-tetradecanol) was emulsified in 80 mL of distilled water at speed of 2000 rpm at 50 °C. Triton 100 (1 g) was added as an emulsifier. Then, 6.25 g MMA, 0.5 mL of ferrous sulfate heptahydrate solution (FSHS), 0.125 g of ammonium persulfate (APS), 1.25 g of ethylene glycol dimethacrylate (EGDM) were added to the emulsion. The stirring speed of the emulsion was decreased to 1000 rpm. Sodium thiosulfate (STS, 0.125 g) and 0.5 g of tert-Butyl hydroperoxide (TBHP) were added and the reaction medium was heated to 85 °C. After 2 hours of stirring at 1000 rpm, the first step of the process was completed. To start the second step of the process, 0.5 g of Triton X100, 6.25 g of MMA, 2.5 g of MA, 0.25 mL of ferrous sulfate heptahydrate solution, 0.0625 g of ammonium persulfate, and 0.625 g of ethylene glycol dimethacrylate were added to the reaction medium. After adding 0.0625 g of sodium thiosulfate and 0.25 g of tert-Butyl hydroperoxide, the reaction was continued at 85 °C for more than 2 hours. Afterward, the nanocapsules were filtered, rinsed with water at 50 °C, and dried at room temperature for analysis. Besides, the production process defined in our previous study was used to produce one walled nanocapsule and named as a one-stage process (OS) [40, 41]. The amount of the materials used in the one-stage production process was given in Table 1. In this process, the polymerization reaction was conducted at 85 °C for 4 hours by stirring at 1000 rpm. The abbreviated names and contents of the nanocapsules were given in Table 1.

2.2.2. Production of core-sheath structured nanofibers

In this study, Nanocapsule-D-TS/PAN core-sheath structured nanofibers were produced by coaxial electrospinning of polyacrylonitrile (PAN) and Nanocapsule-D-TS as the sheath polymer and core material, respectively. The coaxial electrospinning apparatus has an inner spinneret coaxially placed inside an outer one. The basic experimental setup is shown in Figure 1. In the study, 14% PEG core spinneret solution in DMF (w/v) was prepared. Nanocapsules at a specified mass ratio of 40% were mixed in PEG/DMF core solution in order to achieve their homogeneous distribution in the fiber core. To prepare sheath spinneret solution, 6% PAN (w/v) was dissolved in DMF. The outer nozzle syringe pump and the inner syringe pump were set to the flow rate of 2 mL/h and 0.4 mL/h, respectively, to be provided a continuous flow of solutions. Both nozzles were connected to the same electrical potential with the applied voltage of 19.8 kV. The distance between the needle and the collector was fixed at 11 cm.

Before the electrospinning, electrical conductivity of the core and shell solutions was measured. Measurements were performed at 25 °C using a WTW 330 model instrument. In the literature, it was stated that the conductivity of the sheath spinneret solution should be higher than the conductivity of the core spinneret solution in order to make continuous core-sheath structured nanofiber production [42,43]. In the study, electrical conductivity of the sheath spinneret solution (95.5 $\mu S\,cm^{-1}$) was measured as higher as to be contributed to electrospinning of core spinneret solution (7.4 $\mu S\,cm^{-1}$).

Table 1. The abbreviations of the capsules produced in the study and their contents with the method applied

| Production process	Capsule	Wall and core material	Added materials	
			First stage	Second stage
One-stage	Nanocapsule-D-OS	PMMA-co-MA n-dodecanol	12.5 g core 1.5 g of TritonX100 12.50 g MMA 2.5 g MA 0.75 mL FSHS 0.1875 g APS 1.875 g EGDM 0.1875 g STS 0.75 g TBHP	-
	Nanocapsule-T-OS	PMMA-co-MA 1-tetradecanol		-
Two-stage	Nanocapsule-D-TS	PMMA inner PMMA-co-MA outer n-dodecanol	12.5 g core 1 g Triton X-100 6.25 g MMA 0.5 mL FSHS 0.125 g APS 1.25 g EGDM 0.125 g STS 0.5 g TBHP	0.5 g TritonX100 6.25 g MMA 2.5 g MA 0.25 mL FSHS 0.0625 g APS 0.625 g EGDM 0.0625 g STS 0.25 g TBHP
	Nanocapsule-T-TS	PMMA inner PMMA-co-MA outer 1-tetradecanol		
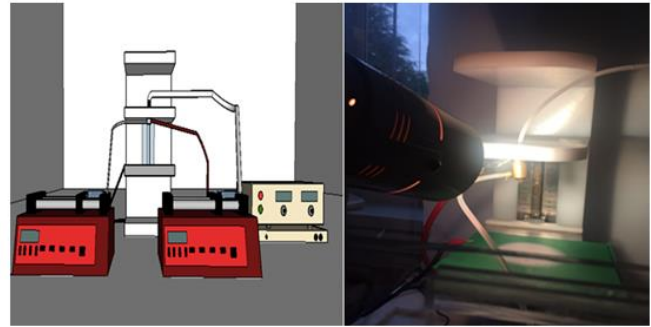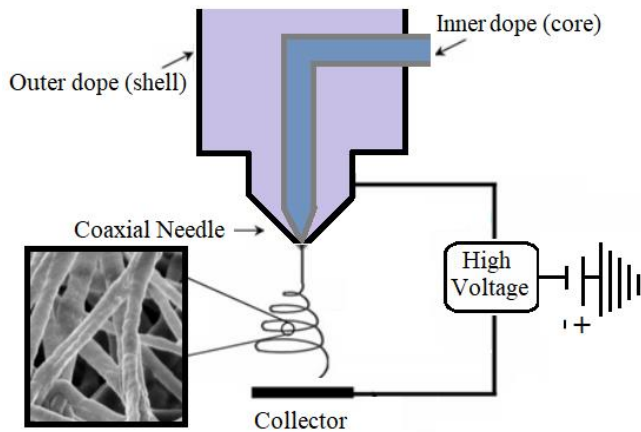
Figure 1. Co-axial electrospinning setup [40].

### 2.2.3. Characterization of the nanocapsules and nanofibers

The morphology and core-shell structure of the nanocapsules were analyzed using transmission electron microscopy (TEM, JEOL JEM2100). In this procedure, one drop of nanocapsule dispersion in the water was dropped onto a copper grid and allowed to dry and examined by TEM. In the study, the thickness of the nanocapsule shell on TEM images was measured using the images of about 50 nanocapsules per each nanocapsule type using an image analysis program. The Fourier transforms infrared (FTIR) transmission spectra of the nanocapsules and nanofibers were recorded between 4000 and 400 cm^{-1} at a resolution of 4 cm^{-1} and a number of scans of 16 using a Perkin Elmer Spektrum BX spectrometer. The spectroscopic analyses of the nanocapsules and nanofibers were performed on KBr disks. The particle size of nanocapsules was measured using a particle size instrument (Malvern MS2000E). Before the measurements, dried capsules were homogenized in the water by an ultrasonic homogenizer (Bandaline Sonuplus UV 2200) for 2 hours. Thermal properties of the nanocapsules and nanofibers such as latent heat storage–releasing capacities and temperatures were measured by differential scanning calorimetry (DSC, Perkin-Elmer Fronter) at a heating–cooling rate of 5 °C/min between -5 °C and + 80 °C under a constant stream of nitrogen at a flow rate of 60 mL/min. In this study, the core material permeability of the nanocapsule shell in an organic solution was investigated. In the test, nanocapsules were immersed in a 10% hexane solution for 24 hours and then washed with hot water, filtered, and dried at room temperature. Their thermal properties were also measured by a DSC instrument. Thermogravimetric analysis (TGA) of the nanoencapsulated fatty alcohols was carried out using a thermal analyzer (Perkin-Elmer TGA7) at a heating rate of 10 °C/min from 25 to 500 °C in nitrogen atmosphere. Differential Thermogravimetry (DTG) was also obtained to determine the maximum rate of weight loss. The morphologies of the nanofibers were investigated using a scanning electron microscope (SEM, LEO 440 Computer Controlled Digital). The surfaces of the nanofibers were coated with gold prior to the imaging.

3. RESULTS AND DISCUSSION

3.1. TEM analysis of the nanocapsules

The core-shell structures of the nanocapsules were examined by TEM analysis. As seen from TEM images given in Figure 2, typical core-shell structured nanocapsules were obtained and the fatty alcohols were encapsulated by a polymeric shell using the one-stage and two-stage emulsion polymerization methods. Spherical-shaped and uniform nano-sized particles were produced successfully. The particle sizes of the nanocapsules on TEM images changed between 200 and 500 nm. Nanocapsule-D-TS and Nanocapsule-D-OS had almost 63 nm and 59 nm shell thicknesses, while Nanocapsule-T-TS and Nanocapsule-T-OS had almost 49 nm and 39 nm shell thickness, respectively (Table 2). It was concluded the shell of the nanocapsules prepared by the two-stage process were thicker although the same amount of shell materials was used in the processes. This might be due to the presence of methacrylic acid comonomer used in wall structure synthesis. Methacrylic acid is a monomer that dissolves in water and swells in the polymerization environment. Addition of water-soluble monomers such acrylic and methacrylic acid into the oil-in-water emulsion medium in microencapsulation processes make the polymerization difficult and decrease the encapsulation efficiency, especially when used in high amounts (10% or more). However, in order to increase the functionality of the microcapsule wall structure, it should be used as much as possible [33]. Here, it was concluded that the addition of the MA co-monomer in the reaction medium at the second step reduced its negative effect on the polymerization process and promoted the formation of a thicker wall structure.
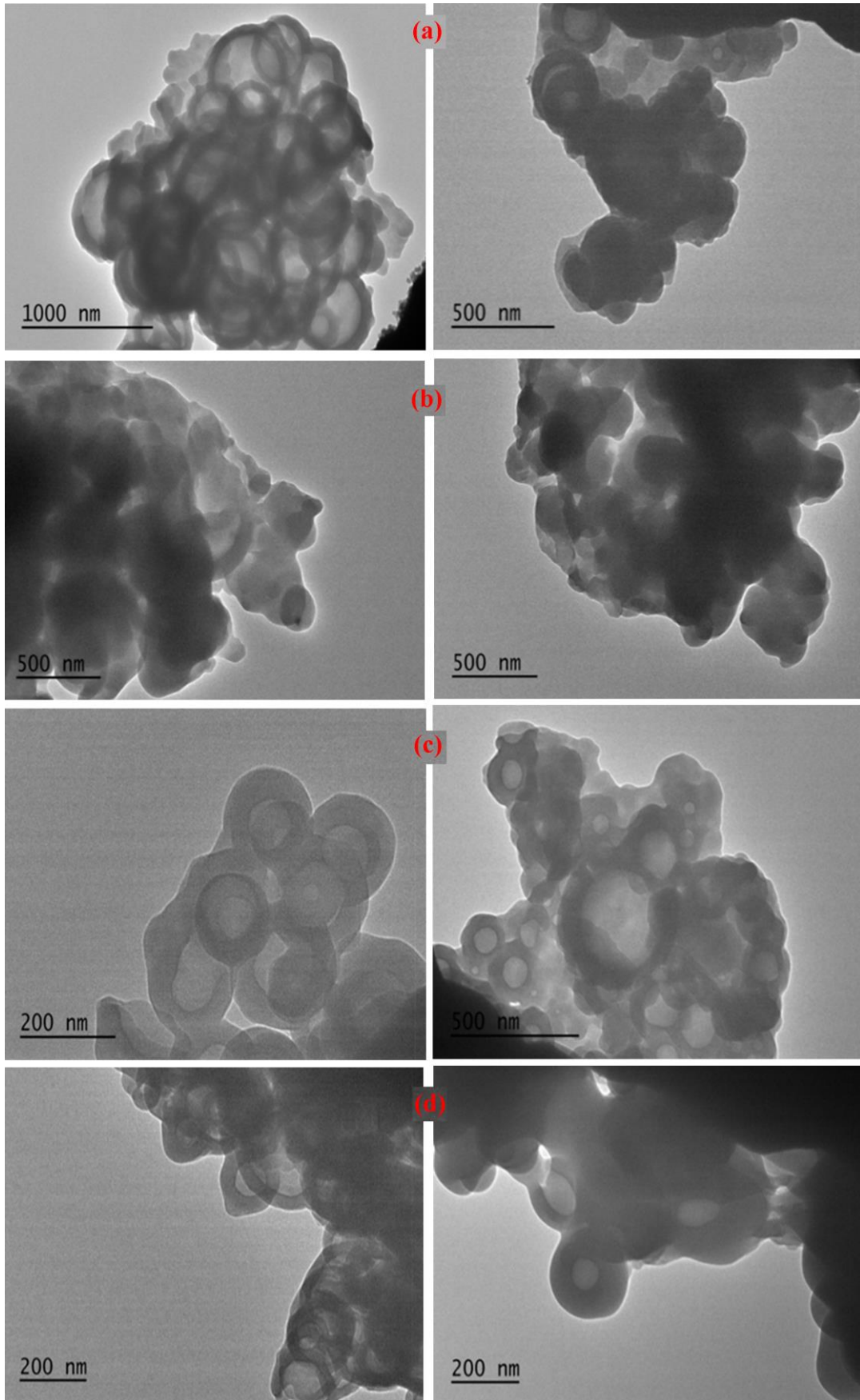
Figure 2. TEM micrographs of the nanocapsules (a: Nanocapsule-D-TS; b: Nanocapsule-D-OS; c: Nanocapsule-T-TS and d: Nanocapsule-T-OS

Table 2. Shell thickness meaurement results of the nanocapsules

Nanocapsules	Shell thickness values			
	Mean	Max.	Min.	CV%
Nanocapsule-D-OS	59	81	32	24.84
Nanocapsule-T-OS	39	44	30	15.58
Nanocapsule-D-TS	63	92	52	16.04
Nanocapsule-T-TS	49	59	37	15.61

3.1.2. FT-IR analysis of the nanocapsules

To study the chemical structures of the nanocapsules, FT-IR spectroscopy analyses were performed. The FTIR spectra of the materials and the information obtained from the FTIR spectra were given in Figure 3 and Table 3. C-H stretching peaks of the n-dodecanol were seen at 2924 cm^{-1} and 2854 cm^{-1} wavelengths in the FT-IR spectra of the Nanocapsule-D-TS and Nanocapsule-D-OS (Figure 3, Table 3). Besides, the medium-strong peaks at 1058-1059 cm^{-1} were belonging to the C-OH vibration of primary alcohol (n-dodecanol) [6,12]. The peaks at 1731 cm^{-1} in the spectra of the nanocapsules were carbonyl peaks formed by overlapping of the carbonyl peaks of the MMA and MA monomers. The peaks at 3390-3360 cm^{-1} in the spectra of nanocapsules were overlapped O-H stretching peaks both of alcohol groups of the n-dodecanol, and carboxylic acid groups of MA monomer. The peaks seen at wavelengths of 1625 cm^{-1} and 1639 cm^{-1}, respectively, in spectra of MMA and MA monomers were the vinyl group (C = C) stretch peaks and were disappeared in the spectra of the nanocapsules [41]. This finding was proof of the polymerization reaction carried out between the MMA and MA monomers. According to the FT-IR spectra of the nanocapsules containing 1-tetradecanol given in Figure 3, the peaks at 2919-2849 cm^{-1} and 2918-2849 cm^{-1} in the FT-IR spectra of the Nanocapsule-T-TS and Nanocapsule-T-OS were C-H stretching peaks of the 1-tetradecanol, which were proofs of the encapsulated 1-tetradecanol. Besides, arising of C-H stretching peaks of 1-tetradecanol at 1466 cm^{-1} in the FT-IR spectra of the nanocapsules were other proofs of its presence in nanocapsule structure [44]. The sharp peaks at a wavelength of 1733 cm^{-1} in the spectra of the nanocapsules were carbonyl (C = O) peaks, which were formed by overlapping of carbonyl peaks in the MA and MMA monomers [41]. The peaks at 3306-3311 cm^{-1} wavelengths in the nanocapsule spectra were O-H stretching peaks of the alcohol group of 1-tetradecanol and the carboxylic acid group of methacrylic acid co-monomer. The peaks at the wavelengths of 1625 cm^{-1} and 1639 cm^{-1} in FT-IR spectra of the MMA and MA monomers,

respectively, were the vinyl group (C = C) stretching peaks of the methacrylic acid and methyl methacrylate monomers [41]. These peaks were disappeared in the nanocapsules FT-IR spectra, which proved that the polymerization between methyl methacrylate and methacrylic acid monomers took place.

3.1.3. DSC analysis of the nanocapsules

To determine the thermal properties of the nanocapsules such as latent heat energy-storing/releasing capacities and temperatures, DSC analysis was performed. The DSC curves of the nanocapsules and the information obtained from the DSC curves were given in Figure 4 and Table 4. As seen from the DSC curves, two peaks were observed in the DSC spectrum during the cooling. This case resulted from liquid-solid and solid-solid phase-change processes of 1-alcohols having low temperature and high temperature crystalline forms. However, solid-solid and solid-liquid transitions during heating were overlapped [45,46]. It was seen from Table 4 that the liquid-solid and solid-solid crystallization temperatures were respectively 19 °C and 9.8 °C for Nanocapsule-D-TS, and 19 °C and 9.2 °C for Nanocapsule-D-OS. It was concluded from DSC analysis that the latent heat storage/releasing capacities of the prepared nanocapsules were very high compared to the findings in the literature [2,6,9-17]. Besides, the enthalpy values of the nanocapsules produced by the two-stage process were measured as higher. As explained before, the presence of a water-soluble MA comonomer in the emulsion medium negatively affects the microencapsulation process and decreases the microencapsulation efficiency. In the two-stage process, only the methyl methacrylate monomer dissolved in the oil phase was used in the first stage of encapsulation. However, in the one-stage process, an MMA monomer, as well as a water-soluble MA monomer, was added to the emulsion during the encapsulation period. Considering this matter, it was concluded that lower enthalpy of the OS-nanocapsules resulted from the adverse effect of the swelling of methacrylic acid monomer in water during the encapsulation process on the encapsulation of the fatty alcohol.

In this study, DSC analysis of nanocapsules was repeated after they were treated with hexane solution to determine the permeability of their shell structure in an organic solution. According to the DSC data given in Table 5, a significant change in their thermal energy storage capacity was observed after treatment with n-hexane for 24 h. They almost lost their latent heat storage capacities in the ratio of 38-40 %. This result meant that the shell structure leaks the core material in the presence of organic solvent n-hexane.

Table 3. FT-IR analysis spectrum information of the nanocapsules

Materials	FT-IR spectrum bands
n-dodecanol	3200-3600 cm^{-1} → O-H stretching peaks 2924 cm^{-1} and 2854 cm^{-1} → C-H stretching peaks 1058-1059 cm^{-1} → Medium peaks are associated with the C-OH vibration of the primary alcohol
1-tetradecanol	3200-3600 cm^{-1} → O-H stretching peaks 2919-2849 cm^{-1} and 2918-2849 cm^{-1} → C-H stretching peaks 1466 cm^{-1} → C-H stretching peak
Methyl methacrylate monomer	1731 cm^{-1} and 1733 cm^{-1} → strerching peak of the carbonyl group 1625 cm^{-1} → C = C (vinly group) peak in monomer
Methacrylic acid monomer	3390-3360 cm^{-1} and 3306-3311 cm^{-1} → Belongs to OH stretching in carboxilic acid group 1731 cm^{-1} and 1733 cm^{-1} → Peak of carbonyl group in the carboxilic acid group 1625 cm^{-1} → C = C (vinly group) peak in monomer
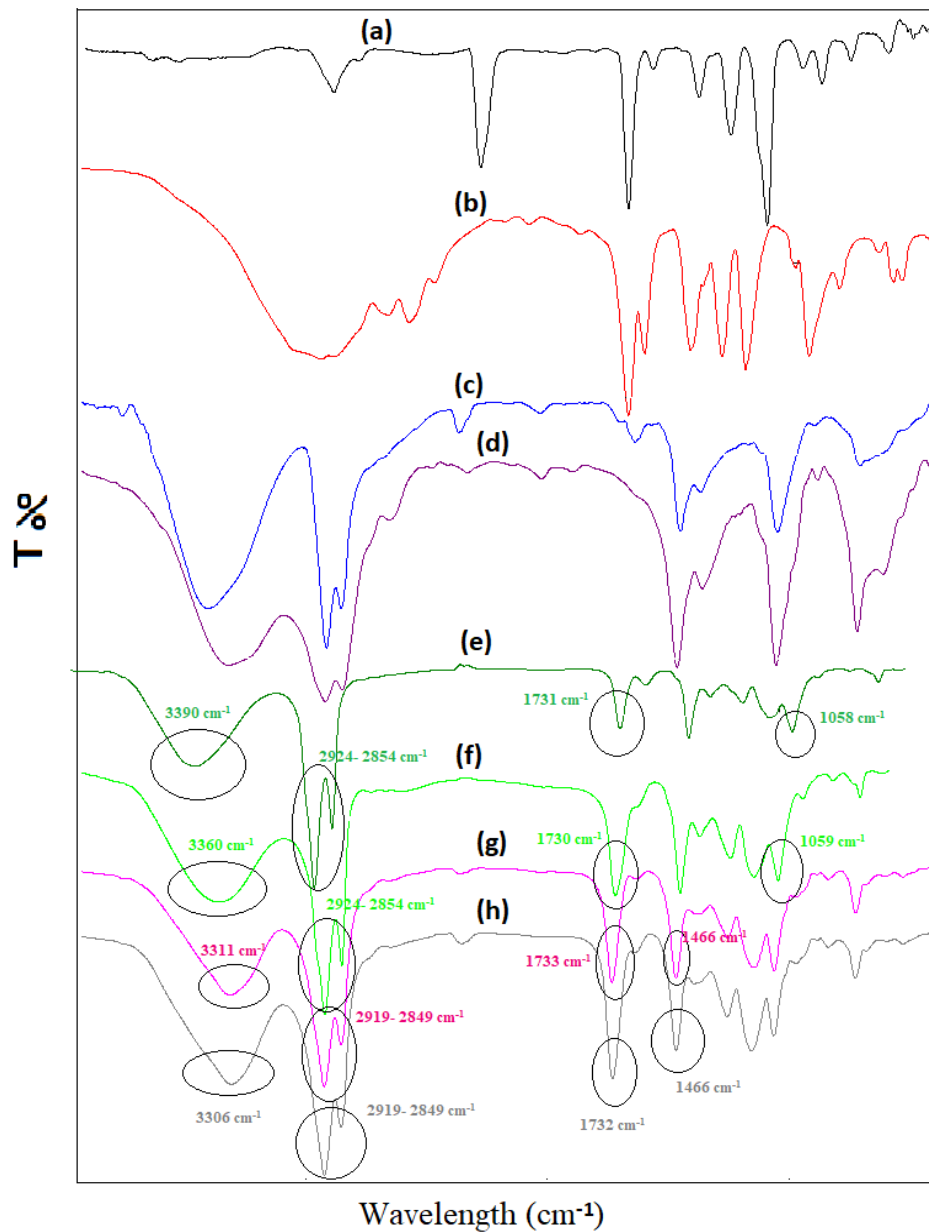
Figure 3. FT-IR spectrum of (a): methyl methacrylate monomer, (b) methacrylic acid monomer, (c) n-dodecanol, (d): 1-tetradecanol, (e):Nanocapsule-D-TS, (f): Nanocapsule-D-OS, (g): Nanocapsule-T-TS, (h): Nanocapsule-T-OS
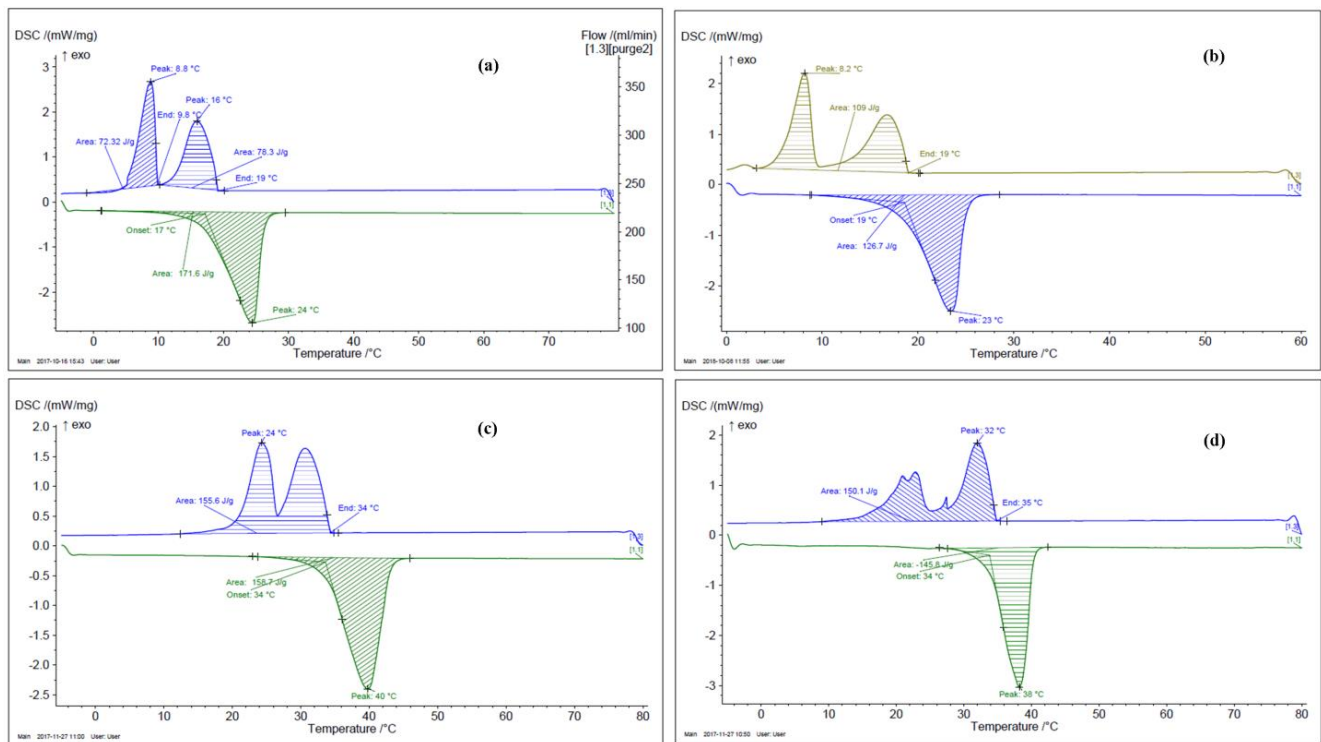
Figure 4. DSC curves of nanoencapsulated n-dodecanol (a: Nanocapsule-D-TS; b: Nanocapsule-D-OS) and 1-tetradecanol (c: Nanocapsule-T-TS; d: Nanocapsule-T-OS)

Table 4. DSC data of the nanocapsules

| Nanocapsule | Melting Temp. (°C) | Melting Enthalpy (J/g) | Crystallization Temp. (°C) | | Total Crystallization Enthalpy Measured During Crystallization (J/g) |
			Solid-Liquid	Solid-Solid	
n-dodecanol	21.58	210.13	20.13	18.23	-209.3
Nanocapsule-D-TS	17	171.6	19	9.8	-150.6
Nanocapsule-D-OS	19	126.7	19	9.2	-101.6
1-tetradecanol	35.5	192.8	35.54	28.97	- 183.4
Nanocapsule-T-TS	34	158.7	34	24	-155.6
Nanocapsule-T-OS	34	145.8	35	24	-150.1

Table 5. DSC analysis results of the nanocapsules treated with hexane

| Nanocapsule | Melting Temp. (°C) | Melting Enthalpy (J/g) | Crystallization Temp. (°C) | | Total Crystallization Enthalpy Measured During Crystallization (J/g) |
			Solid-Liquid	Solid-Solid	
Nanocapsule-T-TS	33	96.01	33	22	-90
Nanocapsule-T-OS	33	89.75	32	21	-84.77

3.1.4. TGA analysis of the nanocapsules

TGA analysis was performed to investigate the thermal stability of the prepared nanocapsules. The TGA curves of the nanocapsules and the information obtained from the TGA curves were given in Figure 5 and Table 6. As seen from the TGA curves given in Figure 5, nanocapsules exhibited two-step thermal degradation. The weight loss of the n-docecanol usually occurs between 140-245 °C as a

typical one-step degradation resulting from its volatilization [2,6,9,11,13]. The first step degradation in the TGA curves of the Nanocapsule-D-TS and Nanocapsule-D-OS nanocapsules started at almost 140 °C corresponding decomposition temperature of n-dodecanol. The weight loss of 76% for the Nanocapsule-D-TS resuled between the temperatures of 148 °C and 200 °C, while the Nanocapsule-D-OS nanocapsules lost 62% of their weight between the

125 °C and 200 °C. The second step thermal degradation, which resulted from the degradation of the shell of the capsules, started at 300 °C for Nanocapsule-D-TS and 290 °C for Nanocapsule-D-OS. The second step weight loss was 21% for the Nanocapsule-D-TS and 25% for the Nanocapsule-D-OS. According to the TGA analysis of the nanocapsules containing 1-tetradecanol, the first-step degradation of the Nanocapsule-T-TS carried out between 148 °C and 290 °C and they lost 75% of their weight. Nanocapsule-T-OS capsules exposed to first step degradation between the 135 °C and 250 °C, and they lost

62% of their weight. The second-step degradation occurred between 290 ° C and 480 °C for the Nanocapsule-T-TS and between 270 ° C and 450 ° C for the Nanocapsule-T-OS. Their weight loss values were 26% and 34%, respectively (Table 6). It was concluded from the TGA analysis results the thermal decomposition temperature of the nanocapsules produced by the two-stage process increased compared to that of the nanocapsules produced by the one-step process. It was concluded that improving the thermal stability of nanocapsules was due to increased wall thickness.
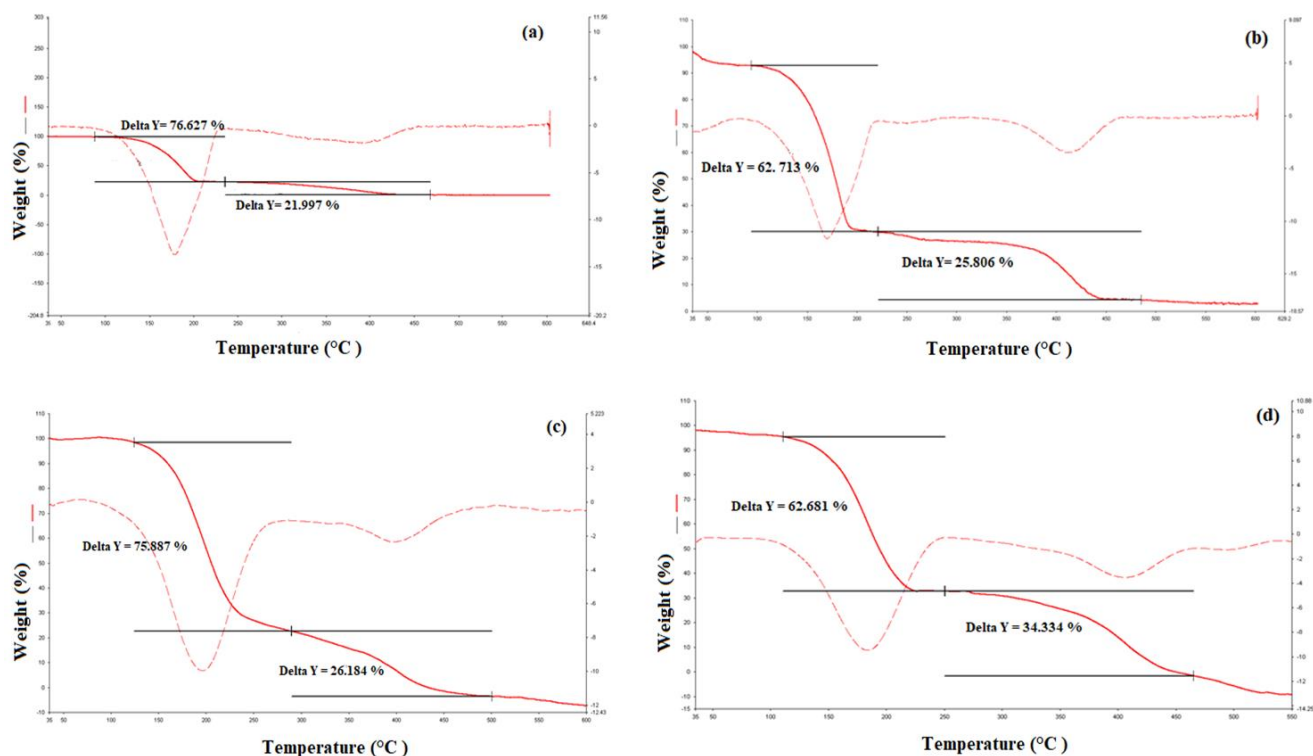
Figure 5. TGA curves of nanoencapsulated n-dodecanol (a: Nanocapsule-D-TS; b: Nanocapsule-D-OS) and nanoencapsulated 1-tetradecanol (c: Nanocapsule-T-TS; d: Nanocapsule-T-OS)

Table 6. TGA data of the nanocapsules

Nanocapsule	Degredation temperature interval (°C)		Weight loss %
Nanocapsule-D-TS	148-200	(Stage 1)	76
	300-425	(Stage 2)	21
Nanocapsule-D-OS	125-200	(Stage 1)	62
	235-440	(Stage 2)	25
Nanocapsule-T-TS	148-290	(Stage 1)	75
	290-480	(Stage 2)	26
Nanocapsule-T-OS	135-250	(Stage 1)	62
	270-450	(Stage 2)	34
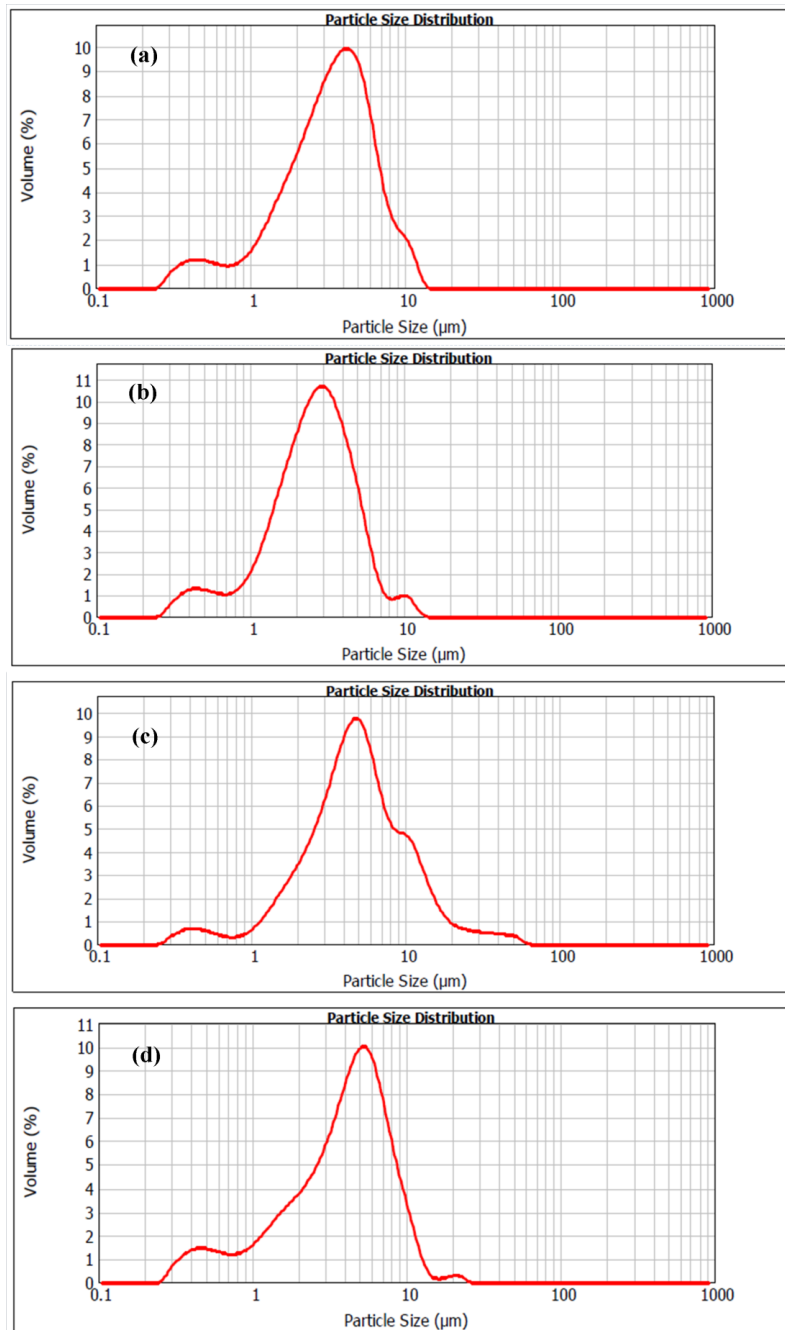
Figure 6. Particle size distribution curves of nanoencapsulated n-dodecanol (a: Nanocapsule-D-TS; b: Nanocapsule-D-OS) and 1-tetradecanol (c: Nanocapsule-T-TS; d: Nanocapsule-T-OS)

3.1.5. Particle size analysis of the nanocapsules

The particle size distribution (PSD) curves of the nanocapsules were given in Figure 6. The nanocapsules exhibited an almost homogenous particle size distribution. However, the average particle sizes measured by particle size instrument were determined bigger than the particle sizes observed as nano-size by TEM micrographics. This finding was consistent with the literature which revealed aggregation of nano-sized capsules during particle size analysis [33,41]. According to the PSD analysis, the mean particle sizes of the Nanocapsule-D-TS and nanocapsule-D-OS were measured as

3.41 μm (uniformity 0.53) and 2.65 μm (uniformity 0.51), respectively. Their particle sizes varied between 1-7 μm. Nanocapsule-T-TS and Nanocapsule-T-OS, containing 1-tetradecanol, had a mean particle size of 4.76 μm (uniformity 0.78) and 4.14 μm (uniformity 0.56), respectively. Their particle sizes varied between 1-12 μm.

3.2.1. SEM analysis of the nanofibers

In order to investigate the possibility of nanocapsule incorporation into the core of the fiber structure without clustering, core/sheath structured nanofiber production was

performed by the coaxial electrospinning method. PAN polymer solution was used as fiber sheath forming polymer and PEG/nanocapsule mixture solution was used for the production of the fiber core. Figure 7b showed the SEM images and fiber diameter distribution diagram of the core/sheath structured bicomponent nanofibers electrospun from PAN and PEG/nanocapsule solutions. Besides, SEM images of used nanocapsules (Nanocapsule-D-TS) and cross-section of the nanofiber web were given in Figure 7 a and Figure 7 c, respectively. According to the SEM images of the nanocapsules given in Figure 7a, the formation of spherical-shaped and uniform nano-sized particles was seen. The SEM images taken from the surface and cross-section of the nanofiber webs showed that nanocapsules were uniformly distributed in the whole body of bicomponent nanofibers without clustering. Both the fiber-like and nanocapsules-like morphologies were retained in the final nanofiber product similar to a rosary-like structure. PAN polymer was wrapped around the nanocapsules like a sheath. The settlement of the nanocapsules in fiber cross-section caused to become rough and coarse fiber morphological structure. However, the diameter distribution of fibers containing nanocapsules was uniform and the mean fiber diameter was almost 210 nm (210 nm, CV % 15,36). The uniformity of fiber diameters was a result of the regular distribution of nanocapsules in the fiber cross-section and was considered to be an indicator that the capsules are placed in the fiber cross-section without clustering.
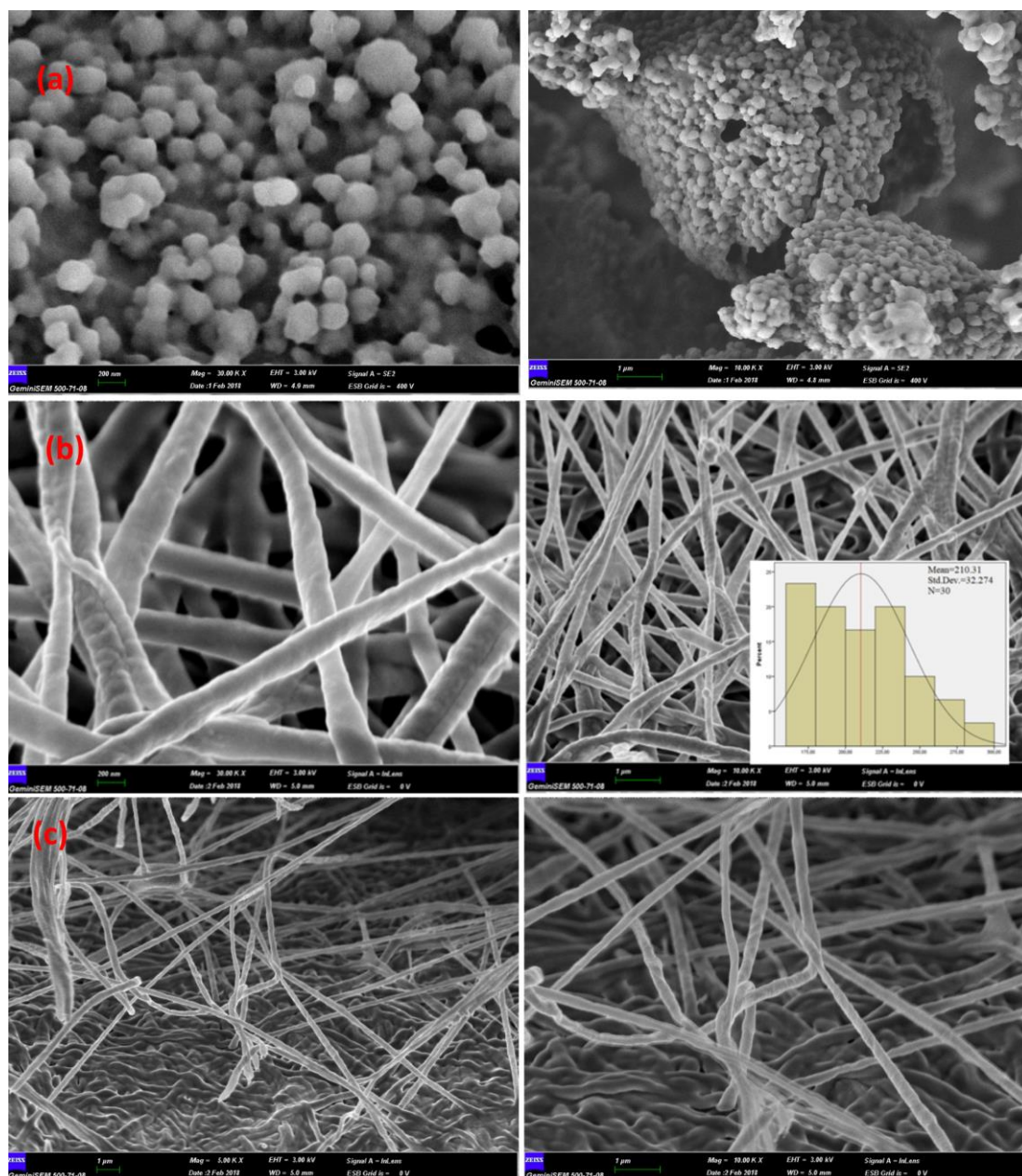
Figure 7. SEM images at different magnifications of the Nanocapsule-D-TS nanocapsules (a) and surface (b) and cross section (c) of the core/sheath structured bicomponent nanofibers

3.2.2. FT-IR analysis of the nanofibers

To investigate the chemical structure of the nanofibers containing Nanocapsule-D-TS capsules produced by the co-axial electrospinning method, FT-IR spectroscopy was used. Figure 8 showed the FTIR transmission spectra of the composite nanofibers, nanocapsules, and pure PAN nanofibers. The findings obtained from the spectra of the materials used in nanofibers production were given in the Table 7. The peak observed at 3425 cm^{-1} in the FT-IR spectrum of the nanofibers was overlapped stretching peaks of O-H groups in polyethylene glycol chains used as core polymer and O-H groups of the encapsulated n-dodecanol. Besides, –C-O stretching peaks at 1110 cm^{-1} and 1240 cm^{-1} wavelengths and C-H bending peak at 1348 cm^{-1} were characteristic peaks of the PEG polymer [21]. The peak at 2243 cm^{-1} in the FT-IR spectrum of nanofibers arose because of the stretching vibrations of the C≡N bonds of the PAN polymer. Besides, the peak at 1454 cm^{-1} was a -CH$_2$ twisting peak in the PAN chains [21,47]. The peaks at 2924 cm^{-1} and 2854 cm^{-1} were -C-H stretching vibrations of the encapsulated n-dodecanol. The peak at 1736 cm^{-1} in the FT-IR spectrum of the nanofibers belonged to the carbonyl groups of copolymer shell (P(MMA-co-MA)) of the nanocapsule.

### 3.2.3. DSC analysis of the nanofibers

DSC curve of the composite core-structured nanofibers containing Nanocapsule-D-TS nanocapsules was given in Figure 9. According to the DSC data, nanofibers stored 19.49 J/g of latent heat at 32.07 °C and released -24.25 J/g of energy at 27.41 °C. However, the melting and solidification temperatures of the nanofibers were found to be quite high compared to those of the capsules added to the structure.

Table 7. FT-IR analysis spectrum information of the nanofibers

Materials	FT-IR spectrum bands
Nanocapsule-D-TS capsule	3390 cm^{-1} → O-H stretching peak of n-dodecanol 2924 cm^{-1} and 2854 cm^{-1} → C-H stretching peaks of n-dodecanol 1731 cm^{-1} → carbonyl peak of the copolymer shell
Polyethylene Glycol (PEG) polymer	3400-3450 cm^{-1} → O-H stretching peak 2890 cm^{-1} is for the C-H aliphatic stretching 1110 cm^{-1} and 1240 cm^{-1} → –C-O stretching peaks 1348 cm^{-1} → C-H bending peak
Polyacrylonitrile (PAN) polymer	2243 cm^{-1} → the stretching peak of the C≡N bonds 1454 cm^{-1} → -CH$_2$ twisting peak
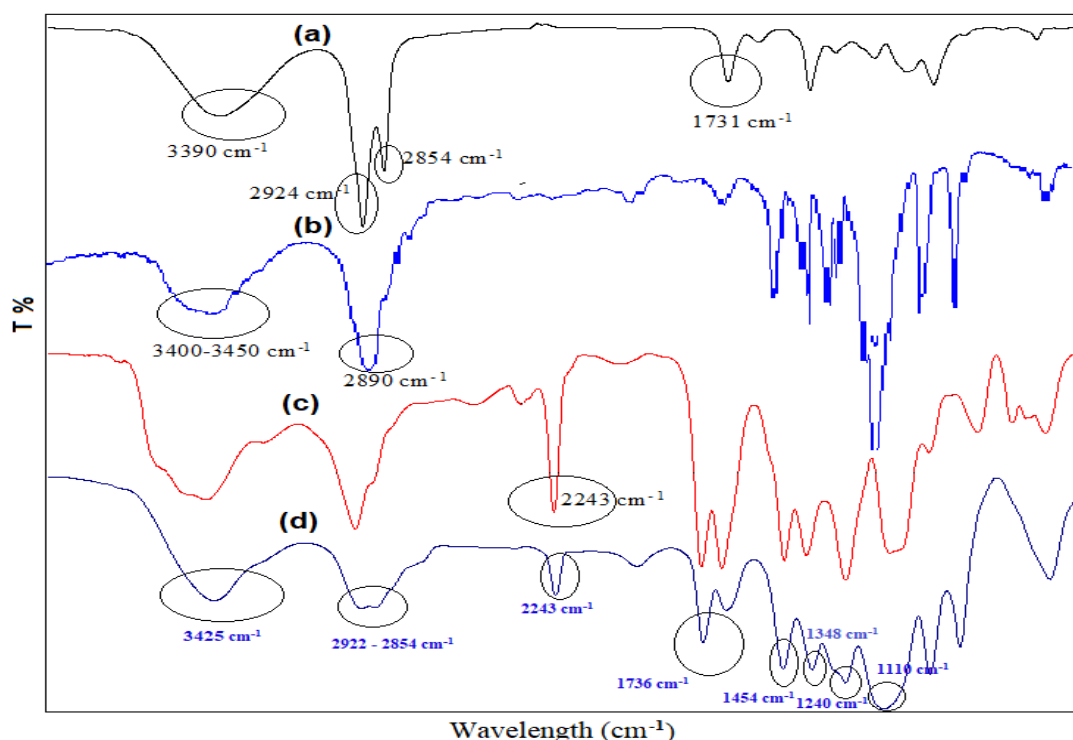
Figure 8. FT-IR spectrum of nanofibers (a: Nanocapsule-D-TS capsule; b:PEG nanofibers c:PAN nanofiber; d) the core/sheath structured bicomponent nanofibers)
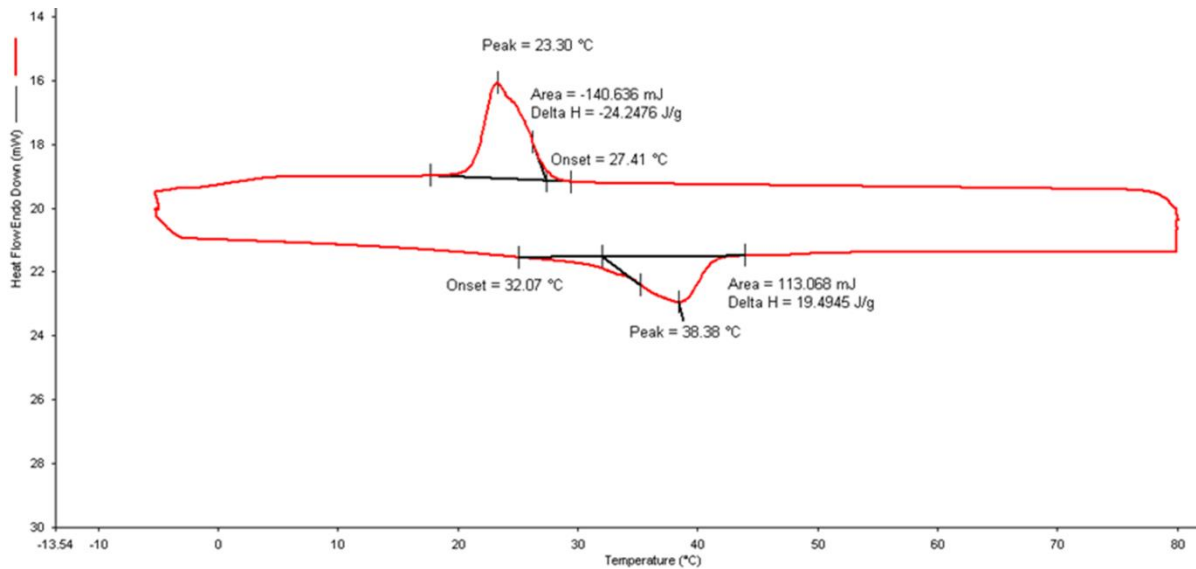
Figure 9. DSC curve of the core-structured composite nanofibers

4. CONCLUSION

In this study, n-dodecanol and 1-tetradecanol were nanoencapsulated for the usage as a thermal energy storage material. Capsule production was carried out using the oil-in-water emulsion polymerization method. Preparation of the nanocapsules with P(MM-co-MA) wall was carried out using conventional emulsion polymerization method and modified two-stage emulsion polymerization method. In the two-stage emulsion polymerization process, firstly MMA monomer was added to the emulsion, and polymerization reaction was started. After the polymerization reaction for 2 hours, both of the MMA and MA monomers were added to the reaction medium to complete the formation of the capsules' wall. According to the FT-IR analysis results, fatty alcohols were encapsulated in a poly(methyl methacrylate-co-methacrylic acid) wall successfully. Nanocapsules had typical core-shell structured, spherical-shaped, uniform nano-sized. The mean particle sizes of the nanoencapsulated n-dodecanol were measured as 3.41 μm for the TS process and 2.65 μm for the OS process. The mean particle sizes of the nanocapsules containing 1-tetradecanol were 4.76 μm for the TS process and 4.14 μm for the OS process. n-Dodecanol encapsulated by the two-stage process solidified at 19°C with the latent heat of 150.6 J/g and melted at 17 °C with the latent heat of 171.6 J/g. Nanocapsules prepared by the one-stage process solidified at 19 °C with the latent heat of 101.6 J/g and melted at 19 °C with the latent heat of 126.7 J/g. Nanoencapsulated 1-tetradecanol using the two-stage process absorbed latent heat of 158.7 J/g at 34 °C and released energy of 155.6 J/g at 34 °C. The nanocapsules prepared by the one-stage process absorbed energy of 145.8 J/g at 34 °C and released energy of 150.1 J/g at 35 °C. The enthalpy values of nanocapsules produced by the two-stage process were measured as higher and reached up to 171 J/g. TGA analysis results showed that the thermal decomposition temperature of the nanocapsules produced by the two-stage process increased compared to that of the nanocapsules produced by the one-step process. It was concluded that improvement in the thermal stability of the nanocapsules was due to increased wall thickness. According to the TEM analysis results, typical core-shell structured, spherical-shaped, uniform nano-sized particles were obtained, and the fatty alcohols were encapsulated using one-stage and two-stage emulsion polymerization processes, successfully. In the study, a nanocapsule sample prepared by the two-stage process was incorporated in polyacrylonitrile nanofibers using a co-axial electrospinning method to fabricate nanofibers with nanocapsule core and PAN sheath. Composite nanofibers having 19 J/g energy storage capacities and unimodal diameter distribution were produced. The surfaces of the nanofibers were rough and coarse but the capsules were placed in the fiber cross-section without clustering. As a result, the nanofibers produced in the study have thermal energy storage capacity, which has the potential to be integrated into technical textile structures such as protective clothing or medical textiles. Nanocapsules prepared in the study also can be evaluated as an additive to be able to apply to fabrics by conventional chemical application methods to produce textiles with thermal energy storage properties. In addition, in the future, studies on the encapsulation of the nanocapsules prepared in this study by various sheath polymers suitable for different usage areas can be conducted.

REFERENCES

1. Sarier N, Onder E. 2012. Organic phase change materials and their textile applications: an overview. *Thermochimica Acta,* 540, 7-60.

2. Geng L, Wang S, Wang R, Luo R. 2016. Facile synthesis and thermal properties of nanoencapsulated n-dodecanol with SiO2 shell as shape-formed thermal energy storage material. *Energy & Fuels,* 30(7), 6153-6160.

3. Ghosh SK. 2006. *Functional coatings by polymer microencapsulation.* Germany: Wiley-VCH Verlag GmbH&Co.KGaA.

4. Alkan C, Sarı A, Karaipekli A, Uzun O. 2009. Preparation, characterization, and thermal properties of microencapsulated phase change material for thermal energy storage. *Solar Energy Materials and Solar Cells,* 93(1), 143-147.

5. Sarı A, Alkan C, Karaipekli A, Uzun O. 2009. Microencapsulated n-octacosane as phase change material for thermal energy storage. *Solar Energy,* 83(10), 1757-1763.

6. Yu F, Chen ZH, Zeng XR. 2009. Preparation, characterization, and thermal properties of microPCMs containing n-dodecanol by using different types of styrene-maleic anhydride as emulsifier. *Colloid Polymer Science,* 287(5), 549–560.

7. Yu F, Chen ZH, Zeng XR. 2009. Preparation and characterization of thermal energy storage microcapsulated n-dodecanol by phase change. *Polymer Materials Science & Engineering,* 25(6), 135-138.

8. Huang R, Li W, Wang J, Zhang X. 2017. Effects of oil-soluble etherified melamine-formaldehyde prepolymers on in situ microencapsulation and macroencapsulation of n-dodecanol. *New Journal of Chemistry,* 41(17), 9424-9437.

9. Su JF, Wang SB, Zhou JW, Huang Z, Zhao YH, Yuan XY, Zhang YY, Kou JB. 2011. Fabrication and interfacial morphologies of methanol–melamine–formaldehyde (MMF) shell microPCMs/epoxy composites. *Colloid Polymer Science,* 289(2), 169-177.

10. Zhang H, Li W, Huang R, Wang J, Zhang X. 2017. Effects of polyvinyl alcohol modification on microstructure, thermal properties and impermeability of microencapsulated n dodecanol as phase change material. *Chemistry Select,* 2(29), 9369-9376.

11. Chen C, Chen Z. Zeng X, Fang X, Zhang Z. 2012. Fabrication and characterization of nanocapsules containing n-dodecanol by miniemulsion polymerization using interfacial redox initiation. *Colloid Polymer Science,* 290(4), 307-314.

12. Chen ZH, Yu F, Zeng XR, Zhang ZG. 2012. Preparation, characterization and thermal properties of nanocapsules containing phase change material n-dodecanol by miniemulsion polymerization with polymerizable emulsifier. *Applied Energy,* 91(1), 7-12.

13. Ma Y, Zong J, Li W, Chen L, Tang X, Han N, Wang J, Zhang X. 2015. Synthesis and characterization of thermal energy storage microencapsulated n-dodecanol with acrylic polymer shell. *Energy,* 87, 86-94.

14. Chen Z, Wang J, Yu F, Zhang Z, Gao X. 2015. Preparation and properties of graphene oxide-modified poly(melamine-formaldehyde) microcapsules containing phase change material n-dodecanol for thermal energy storage. *Journal of Materials Chemistry A,* 3(21), 11624-11630.

15. Yu F, Chen ZH, Zeng XR, Gao XN, Zhang ZG. 2015. Poly(methyl methacrylate) copolymer nanocapsules containing phase change material (n-dodecanol) prepared via miniemulsion polymerization. *Journal of Applied Polymer Science,* 132(31), 1-7.

16. Li W, Zong J, Huang R, Wang J, Wang N, Han N, Zhang X. 2016. Design, controlled fabrication and characterization of narrow-disperse macrocapsules containing Micro/NanoPCMs. *Materials & Design,* 99, 225-234.

17. Wu N, Xu L, Zhang C. 2018. The influence of emulsifiers on preparation and properties of microencapsules of melamine–urea–formaldehyde resins with n-dodecanol as phase change material. *Advances in Polymer Technology,* 37(8), 3492-3498.

18. Cai Y, Ke H, Lin L, Fei X, Wei Q, Song L, Fong H. 2012. Preparation, morphology and thermal properties of electrospun fatty acid eutectics/polyethylene terephthalate form-stable phase change ultrafine composite fibers for thermal energy storage. *Energy Conversion and Management,* 64, 245- 255.

19. Cai Y, Zong X, Zhang J, Du J, Dong Z, Wei Q, Zhao Y, Chen Q, Fong H. 2014. The improvement of thermal stability and conductivity via incorporation of carbon nanofibers into electrospun ultrafine composite fibers of lauric acid/polyamide 6 phase change materials for thermal energy sorage. *International Journal of Green Energy,* 11(8), 861-875.

20. Sun SX, Xie R, Wang XX, Wen GQ, Liu Z, Wang W, Ju XJ, Chu LY. 2015. Fabrication of nanofibers with phase-change core and hydrophobic shell, via coaxial electrospinning using nontoxic solvent. *Journal of Materials Science,* 50(17), 5729-5738.

21. Noyan ECB, Onder E, Sarier N, Arat R. 2018. Development of heat storing poly(acrylonitrile) nanofibers by coaxial electrospinning. *Thermochimica Acta,* 662, 135-148.

22. Hu W, Yu X. 2014. Thermal and mechanical properties of bio-based PCMs encapsulated with nanofibrous structure. *Renewable Energy,* 62, 454- 458.

23. Zdraveva E, Fang J, Mijovic B, Lin T. 2015. Electrospun poly(vinyl alcohol)/phase change material fibers: morphology, heat properties, and stability. *Industrial & Engineering Chemistry Research,* 54(35), 8706-8712.

24. Lu Y, Xiao X, Zhan Y, Huan C, Qi S, Cheng H, Xu G. 2018. Core-sheath paraffin-wax-loaded nanofibers by electrospinning for heat storage. *ACS Applied Materials & Interfaces,* 10(15), 12759-12767.

25. Lu Y, Xiao X, Fu J, Huan C, Qi S, Zhan Y, Xu G. 2019. Novel smart textile with phase change materials encapsulated core-sheath structure fabricated by coaxial electrospinning. *Chemical Engineering Journal,* 355, 532-539.

26. McCann JT, Marquez M, Xia Y. 2006. Melt coaxial electrospinning: A versatile method for the encapsulation of solid materials and fabrication of phase change nanofibers. *Nano Letters,* 6(12), 2868- 2872.

27. Chen C, Zhao Y, Liu W. 2013. Electrospun polyethylene glycol/cellulose acetate phase change fibers with core-sheat

sctructure for thermal energy storage. *Renewable Energy, 60, 222.-225.*

28. Van Do C, Nguyen TTT, Park JS. 2013. Phase-change core/shell structured nanofibers based on eicosane/poly (vinylidene fluoride) for thermal storage applications. *Korean Journal of Chemical Engineering, 30(7), 1403-1409.*

29. Dang, TT, Nguyen TTT, Chung OH, Park JS. 2015. Fabrication of form-stable poly(ethylene glycol)-loaded poly(vinylidene fluoride) nanofibers via single and coaxial electrospinning. *Macromolecular Research, 23(9), 819-829.*

30. Sun SX, Xie R, Wang XX, Wen GQ, Liu Z, Wang W, Ju XJ, Chu LY. 2015. Fabrication of nanofibers with phase change core and hydrophobic shell, via coaxial electrospinning using nontoxic solvent. *Journal of Materials Science, 50(17), 5729–5738.*

31. Sarier N, Arat R, Menceloğlu Y, Önder E, Boz EC, Oğuz O. 2016. Production of PEG grafted PAN copolymers and their electrospun nanowebs as novel thermal energy storage materials. *Thermochimica Acta, 643, 83- 93.*

32. Babapoor A, Karimi G, Golestaneh SI, Mezjin MA. 2017. Coaxial electro-spun PEG/PA6 composite fibers: Fabrication and characterization. *Applied Thermal Engineering, 118, 398- 407.*

33 Alkan C, Alay Aksoy S, Altun Anayurt R. 2015. Synthesis of poly(methyl methacrylate-co-acrylic acid)/n-eicosane microcapsules for thermal comfort in textiles, *Textile Research Journal, 85(19), 2051–2058.*

34. Chang CC, Tsai YL, Chiu JJ, Chen H. 2009. Preparation of phase change materials microcapsules by using PMMA network-silica hybrid shell via sol-gel process. *Journal of Applied Polymer Science, 112(3), 1850- 1857.*

35. Sarı A, Alkan C, Karaipekli A. 2010. Preparation, characterization and thermal properties of PMMA/ n-heptadecane microcapsules as novel solid-liquid microPCM for thermal energy storage. *Applied Energy, 87(5), 1529-1534.*

36. Qiu X, Li W, Song G, Chu X, Tang G 2012. Microencapsulated n-octadecane with different methylmethacrylate-based copolymer shell as phase change materials for thermal energy stgorage. *Energy, 46(1), 188-199.*

37. Wang Y, Shi H, Xia TD, Zhang T, Feng HX. 2012. Fabrication and performances of microencapsulated paraffin composites with polymethylmethacrylate, *Materials Chemistry and Physics, 135(1), 181-187.*

38. Sarı A, Alkan C, Biçer A, Altuntas A. Bilgin C. 2014. Micro/nanoencapsulated n-nonadecane with poly(methyl methacrylate) shell for thermal energy storage. *Energy Conversion and Management, 86, 614–621.*

39. Al-Shannaq R, Farid M, Al-Muhtaseb S, Kurdi J. 2015. Emulsion stability and cross-linking of PMMA microcapsules containing phase change materials. *Solar Energy Materials and Solar Cells, 132, 311-318.*

40. Özkayalar S. 2019. Production and textile application of double-walled nano and microcapsules with phase change material core (Master's thesis). Available from http://tez.sdu.edu.tr/Tezler/TF04267.pdf.

41. Alay Aksoy S, Alkan C, Tözüm MS, Demirbağ S, Altun Anayurt R, Ulcay Y. 2017. Preparation and textile application of poly(methyl methacrylate-co-methacrylic acid)/n-octadecane and n-eicosane microcapsules. *The Journal of the Textile Institute*, 108(1), 30-41.

42. Moghe AK, Gupta BS. 2008. Co-axial electrospinning for nanofiber structures: preparation and applications. *Polymer Reviews, 48(2), 353-377.*

43. Onder E, Sarier N, Arat R. 2017. The manufacture of organic carbonate-poly (methyl ethylacrylate) nanowebs with thermal buffering effect. *Thermochimica Acta, 657, 170-184.*

44. Wang H, Gui P, Zhu Y, Hu S. 2020. Preparation and characterization of poly(melamine-urea-formaldehyde) tetradecanol microcapsules coated with silver particles. *Journal of Wuhan University of Technology-Material Science Edition, 35(2), 327-334.*

45. Panák O, Držková M, Svoboda R, Gunde MK. 2017. Combined colorimetric and thermal analyses of reversible thermochromic composites using crystal violet lactone as a colour former. *Journal of Thermal Analysis and Calorimetry*, 127(1), 633-640.

46. Tozum MS, Alay-Aksoy S, Alkan C. 2018. Microencapsulation of three-component thermochromic system for reversible color change and thermal energy storage. *Fiber Polymers, 19(3), 660- 669.*

47. Ribeiro RF, Pardini LC, Alves NP, Brito CAR. 2015. Thermal stabilization study of polyacrylonitrile fiber obtained by extrusion. *Polimeros, 25(6), 523–530.*